Atomic Force Microscopy Imaging of DNA Covalently Immobilized on a Functionalized Mica Substrate

Luda S. Shlyakhtenko,*# Alexander A. Gall,§ Jeffrey J. Weimer,¶ David D. Hawn,‖ and Yuri L. Lyubchenko* **
*Department of Microbiology, Arizona State University, Tempe, Arizona 85287-2701; #BioForce Laboratory, Inc., Ames, Iowa 50010-8277; §Epoch Pharmaceuticals, Inc., Redmond, Washington 98052; ¶Chemistry/Chemical & Materials Engineering, University of Alabama at Huntsville, Huntsville, Alabama 35899; ‖Analytical Sciences Division, Dow Chemical Company, Midland, Michigan; and **Department of Biology, Arizona State University, Tempe, Arizona 85287 USA

ABSTRACT A procedure for covalent binding of DNA to a functionalized mica substrate is described. The approach is based on photochemical cross-linking of DNA to immobilized psoralen derivatives. A tetrafluorphenyl (TFP) ester of trimethyl psoralen (trioxalen) was synthesized, and the procedure to immobilize it onto a functionalized aminopropyl mica surface (AP-mica) was developed. DNA molecules were cross-linked to trioxalen moieties by UV irradiation of complexes. The steps of the sample preparation procedure were analyzed with x-ray photoelectron spectroscopy (XPS). Results from XPS show that an AP-mica surface can be formed by vapor phase deposition of silane and that this surface can be derivatized with trioxalen. The derivatized surface is capable of binding of DNA molecules such that, after UV cross-linking, they withstand a thorough rinsing with SDS. Observations with atomic force microscopy showed that derivatized surfaces remain smooth, so DNA molecules are easily visualized. Linear and circular DNA molecules were photochemically immobilized on the surface. The molecules are distributed over the surface uniformly, indicating rather even modification of AP-mica with trioxalen. Generally, the shapes of supercoiled molecules electrostatically immobilized on AP-mica and those photocross-linked on trioxalen-functionalized surfaces remain quite similar. This suggests that UV cross-linking does not induce formation of a noticeable number of single-stranded breaks in DNA molecules.

INTRODUCTION

Immobilization of the sample is a key step toward successful imaging of biological molecules with atomic force microscopy (AFM). A number of sample preparation techniques were developed for reliable AFM imaging of DNA. Vesenka, Bustamante, and co-workers (Bustamante et al., 1992, 1994; Vesenka et al., 1992; Hansma et al., 1992; Bezanilla et al., 1994) improved the method of ionic treatment of mica suggested earlier for preparation the samples for TEM (Brack, 1981). In this approach, a mica surface is treated with multivalent ions (e.g., Mg^{2+}) to increase its affinity to DNA, which is held in place strongly enough to permit reliable imaging with AFM. Untreated mica was later shown to be useable as well, provided that DNA is deposited in solutions containing a magnesium salt. Other di or trivalent cations are used for immobilization of DNA on mica surfaces (Hansma and Laney, 1996). In addition to imaging of DNA, this cation-assisted method was successfully applied to studies of complexes of DNA with proteins (reviewed in Bustamante et al., 1994; Bustamante and Rivetti, 1996). A well-known electron microscopic (EM) procedure, cytochrome *c*-mediated spreading technique (Delain and Le Cam, 1995) was applied for mounting the samples on carbon-coated mica substrates for their imaging with AFM (Yang et al., 1992). Schaper et al. (1993) implemented another EM technique based on the spreading action of benzyldimethylalkylammonium chloride (BAC; Delain and Le Cam, 1995). Gold substrates can be activated by self-assembled monolayers of thiols for reliable immobilization of DNA (Hegner et al., 1993). Nonmodified cover glass appeared to be a good substrate for binding chromatin, although the rinsing step (to remove nonbound material and salt components) should be done gently and the dried sample should be imaged immediately (Allen et al., 1993). We have worked on a quite different approach (Lyubchenko et al., 1992, 1993a, b, 1995, 1996) based on the use of aminopropyltriethoxysilane (APTES) to functionalize the mica surface with amino groups (AP-mica). The conditions for uniform and smooth modification of the surface allowing reliable imaging of DNA were found (Lyubchenko et al., 1992, 1996). The main advantage of this approach is that reproducible imaging of DNA and nucleoprotein complexes can be done in a very broad range of environmental conditions (Lyubchenko et al., 1996, 1997; Bezanilla et al., 1995; Lyubchenko and Shlyakhtenko, 1997; Lyubchenko and Lindsay, 1998; Shlyakhtenko et al., 1998; Herbert et al., 1998).

A common feature of the methods listed above is that they afford relatively weak interactions between the surface and the sample. This has allowed several groups to observe the dynamics of a number of systems with AFM. The process of enzymatic DNA degradation was observed directly by Bezanilla et al. (1994), and direct movement of RNA polymerase along the DNA template has been observed by Kasas et al., (1997). Segmental mobility of supercoiled DNA and dynamics of cruciform arms imaged with AFM in buffer solutions have been reported in our

Received for publication 28 December 1998 and in final form 8 April 1999.
Address reprint requests to Dr. Yuri Lyubchenko, Department of Microbiology, Arizona State University, Box 872701, Tempe, AZ 85287-2701. Tel.: 602-965-8430; Fax: 602-965-0098; E-mail: yuri.lyubchenko@asu.edu.

0006-3495/99/07/568/09 $2.00

recent papers (Lyubchenko and Shlyakhtenko, 1997; Shlyakhtenko et al., 1998).

Comparison with the cases where weak binding is advantageous shows that many examples exist when a strong binding is needed. Various immobilization schemes have been proposed for such cases. A highly charged cationic bilayer assembled on the mica surface was suggested as a substrate for holding of DNA (Mou et al., 1995). DNA pitch was revealed in AFM images, but supercoiled DNA molecules adopted a rather unusual configuration on this surface. The covalent attachment of thiol-modified DNA oligomers to self-assembled monolayer silane films on fused silica and oxidized silicon substrates was described in Chrisey et al. (1996) and Lee et al. (1996). Similar immobilization chemistry via a flexible cross-linker has been developed in Schindler's group for immobilization proteins of different types (Haselgrebler et al., 1995; Hinterdorfer et al., 1996).

Here we report an alternative approach based on covalent photochemical cross-linking of DNA to a trimethyl derivative of psoralen (trioxalen) immobilized onto a mica surface coated with aminopropyltriethoxysilane (AP-mica). Psoralens are bifunctional photoreagents that intercalate into double-stranded nucleic acid and cross-link to pyrimidine bases after irradiation with soft UV light (320–400 nm; reviewed in Cimino et al., 1985). X-ray photoelectron spectroscopy (XPS) and AFM show that an AP-mica surface derivatized with trioxalen is capable of binding DNA. After UV cross-linking, the DNA molecules remain on the surface and are able to withstand thorough washing of physisorbed molecules with SDS. Observations with AFM showed that the photochemically immobilized molecules are severely kinked. The kinks are likely induced by formation of interstrand cross-links.

METHODS

Synthesis of derivatized trioxalen reagent (TFP-trioxalen)

The synthesis of 2,3,5,6-tetrafluorophenyl 3-(4,5′,8-trimethylpsoralen-4′-yl)propionate (TFP-trioxalen, **1**) is shown schematically in Fig. 1. A suitable linker arm was introduced into trioxalen using common synthetic techniques. By coupling of trioxalen derivative **2** with diethyl malonate and subsequent hydrolysis and decarboxylation, trioxalen carboxylic acid derivative **6** was obtained in a high overall yield. This acid was converted into an activated ester **1** using 2,3,5,6-tetrafluorophenyl trifluoroacetate reagent (**7**) (Gamper et al., 1993). A detailed procedure for the synthesis of TFP-trioxalen is also described at http://www.bioforcelab.com/.

Preparation of TO-AP-mica

An AP-mica surface was obtained by vapor deposition of APTES at ambient conditions according the procedure described elsewhere (Lyubchenko et al., 1992, 1993a, b, 1996; Lyubchenko and Lindsay, 1998). Dry trioxalen powder was dissolved in dimethylformamide (Aldrich, Milwaukee, WI) to a final concentration of 5 mM and immediately covered with foil to minimize light exposure. A strip of AP-mica was immersed in 5 mM of the trioxalen solution in dimethylformamide (1.5 ml Eppendorf tube), and the tube was then covered with foil and left overnight. After reaction with trioxalen, the strip of mica was thoroughly washed in dimethylformamide solution to remove nonspecifically bound trioxalen. Usually, the mica strip was submerged in dimethylformamide solution at least 20–30 times. After washing in dimethylformamide, the mica strip was washed with deionized water (ModuLab, Continental System Corp., San Antonio, TX) and dried with argon.

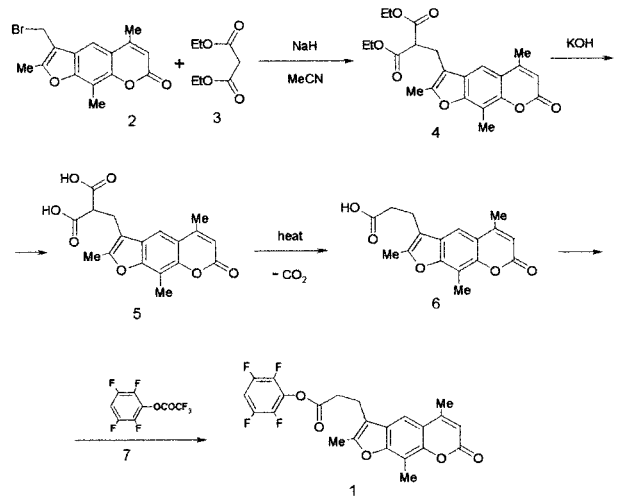

FIGURE 1 The scheme of synthesis of 2,3,5,6-tetrafluorophenyl 3-(4,5′,8-trimethylpsoralen-4′-yl)propionate (TFP-trioxalen, **1**).

Immobilization of DNA on TO-AP-mica

A solution of DNA in TE buffer (10 mM Tris, 1 mM EDTA) was placed onto a TO-AP-mica piece and left for 2 min under a UV lamp (Model UVL-21, VWR, Durham, NC) at 365 nm wavelength. The specimens were then thoroughly rinsed with water and placed into 2% SDS solution for at least 30 min to remove noncovalently bound DNA. SDS was previously found to be very effective for washing noncovalently bound proteins from AP-glutaraldehyde surfaces (Vandenberg et al., 1991). The specimens were then rinsed with water and dried with argon. As an alternative to SDS, concentrated salt solutions (2 M NaCl) and chloroquine (2 μg/ml) were tested as well. In control experiments in which UV irradiation was omitted, DNA deposition was performed for 2 min at ambient conditions.

Deposition of DNA on AP-mica

The samples were prepared similarly to a method described elsewhere (Lyubchenko et al., 1992, 1993a, b, 1995). Briefly, 10 μl DNA (0.5 μg/ml) in TE buffer plus 100 mM NaCl was placed onto pieces of AP-mica for 2 min, rinsed with deionized water, and argon-dried.

Imaging with AFM

The AFM images were taken in air with a MultiMode SPM instrument equipped with a D-scanner (Digital Instruments, Inc., Santa Barbara, CA) operating in TappingMode. NanoProbe TESP probes (Digital Instruments, Inc.) and conical sharp silicon tips (K-TEK International, Portland, OR) were used for imaging in air. The typical tapping frequency was 240–280 KHz for TESP tips and 340–380 KHz for the K-TEK probes, and the nominal scanning rate was 2–3 Hz.

Analysis with XPS

Analysis with XPS was done on one sample of each specimen: freshly cleaved mica, AP-mica, TO-AP-mica, DNA/TO-AP-mica, and DNA/AP-

mica. Spectra were obtained at 90° and 30° takeoff angles using a Kratos Axis 165 system (Kratos Analytical, Chesnut Ridge, NY) and monochromatic Al Kα x-rays at 225 W (14 kV, 15 mA). A charge neutralizer at a nominal bias of -1.15 V was used to compensate for peak shifting. Pass energies of 80 eV and 20 eV were used for survey and high-resolution scans, respectively. Compositional information was taken from survey and high-resolution scans. Postprocessing of the high-resolution XPS spectra for peak fitting and display was done off-line using analysis and manipulation routines developed for Igor Pro (WaveMetrics). The peaks were found to be shifted to low binding energy (BE) due to overbias of the charge neutralizer. In each set of high-resolution spectra, the peaks were shifted back (to higher BE) to bring the K 2p peak to 293.0 eV, which is representative of K^+ in KCl, KBr, or KF (Briggs and Seah, 1990). The XPS results discussed below are not dependent on the absolute positions of the peaks in the spectra. During peak fitting, the relative peak areas of N 1s component peaks were also found to be sensitive to the initial peak positions and half-widths used in the fitting process. In order to obtain a representative sample of the uncertainties, four separate fitting trails were done. The peak parameters were freely fit on the N 1s peak at 90° takeoff from AP-mica. On each subsequent N 1s spectrum (from a different sample), this base set was used with fixed position and half-width for the first trial, with fixed position only for the second trial, and with fixed half-width only for the third trial. The fourth peak fitting trial was run with all three parameters (positions, half-widths, and heights) freely variable.

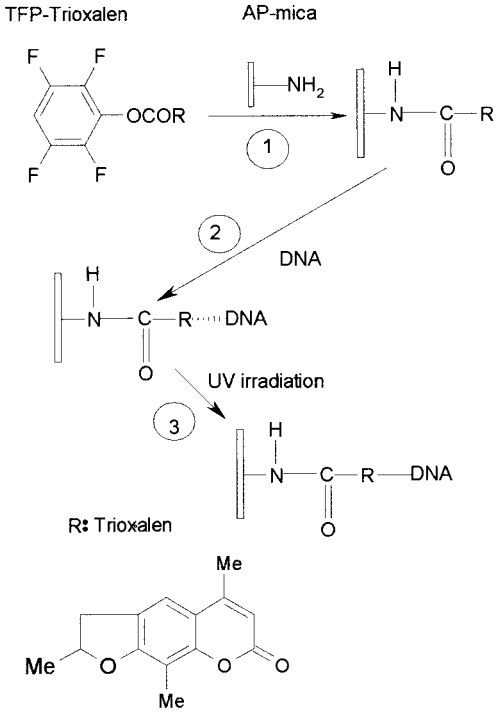

FIGURE 2 The scheme of preparation of the samples studied in this work. TFP trioxalen was synthesized according the scheme shown in Fig. 1.

RESULTS AND DISCUSSION

DNA immobilization

Our approach to covalent DNA immobilization is based on the ability of intercalated psoralens to bind covalently to DNA bases after irradiation with soft UV (Cimino et al., 1985). Psoralens form stable intermolecular complexes reacting primarily with thymidine in double-stranded DNA, although a minor reaction with cytosine also occurs. Note that psoralen-mediated photocross-linking is widely used for covalent binding of oligonucleotides to DNA targets for various purposes, including for mapping of DNA tracts in left-handed Z-conformation with AFM (Pfannschmidt et al., 1996). The three-step procedure is shown schematically in Fig. 2. We used derivatized tri-methylpsoralen (trioxalen) because methylated psoralens are much more reactive than their unsubstituted compounds (Cimino et al., 1985). Tetrafluorphenyl ester of trioxalen (**1**; see Fig. 1) was synthesized for attaching trioxalen to the aminopropyl AP-mica surface.

AP-mica prepared by vapor deposition at ambient conditions (Lyubchenko et al., 1992, 1993a, 1995, 1996) is treated with derivatized trioxalen (TO), which can bind to the amino surface covalently through the reaction of amines with the TFP group of the reagent. DNA solution is placed onto pieces of activated AP-mica to allow the complex to form (step 2). UV irradiation at 365 nm (step 3) leads to covalent bonding of trioxalen to DNA through formation of the monoadducts and diadducts (cross-links) between pyrimidines and intercalated trioxalen. Both adducts are chemically stable unless the complex is exposed to short-wavelength UV light.

XPS analysis

Analytical surface spectroscopic techniques such as XPS are widely applied to characterize the composition and chemistry of surfaces (Briggs and Seah, 1990). They have been used for monitoring the process of surface modification, including those for preparation of substrates or probes for scanning probe microscopy (Lyubchenko et al., 1991; Rabke et al., 1994; Lee et al., 1996) and to characterize the binding of alkylamines to different surfaces (e.g., Moses et al., 1978; Nagasaki et al., 1996). The primary information obtained from XPS is the atomic concentrations of elements in the topmost 10 nm of the surface. Additional information about oxidation or hybridation states can be obtained from high-resolution scans of elemental peaks in the spectra. Analysis at shallow angles (30°) is more surface-sensitive than analysis at normal takeoff angles.

Atomic concentrations of carbon, oxygen, potassium, silicon, and nitrogen were determined from high-resolution XPS scans at the 90° takeoff angle of the respective peaks. The results are given in Table 1. The trend is toward

TABLE 1 Atomic concentrations of elements on samples as determined from XPS survey scans at 90° takeoff angle

Sample	C	O	K	Si	N
Mica	9.7	70	5.2	15	0.3
TO-mica	14	65	3.9	15	1.7
DNA/TO-mica	23	56	3.2	15	2.1
AP-mica	12	66	5.2	16	1.3
DNA/AP-mica	19	59	3.6	17	1.9

increasing carbon concentration at each step of the modification procedure. The relative concentration of silicon is almost constant at all steps, indicating that the increase in number of silicon atoms due to binding of aminopropyltriethoxysilane to mica is very low in comparison with the bulk amount of silicon already measured from the mica. The data are consistent with fluorescence measurements of the surface concentrations of AP groups (Lyubchenko and Shlyakhtenko, 1997). This behavior will occur for thin, uniform layers of silane (under ~2–5 nm thick) or patchy layers of silane, where the XPS measurements can also probe through to the underlying mica. The high-resolution scans at 90° takeoff angle for O 1s, C 1s, and Si 2p peaks of bare mica and AP-mica are shown in Fig. 3. The peak shapes and their positions were comparable for all five specimens. The only noticeable change in surface chemistry in this regard was a decrease in the high BE peak typically associated with carbonyl or carbonate carbons when mica was coated with APTES, as seen in Fig. 3 at ~289 eV. This is likely due to a displacement of these otherwise common carbon contaminates by the silane molecules, as has been seen with XPS to occur on silylation of copper surfaces (Mishra and Weimer, 1995).

The positions for O 1s and Si 2p peaks were compared for bare mica and AP-mica. The BE differences (O 1s − Si 2p) were 429.15 ± 0.05 eV and 429.43 ± 0.03 eV for the mica and AP-mica spectra, respectively. Deposition of the APTES leads to a further separation of the O 1s and Si 2p peaks by ~0.2–0.3 eV. Measurements of O 1s and Si 2p peak positions in siloxane and silicate compounds has given separation values of <429.6 eV for silicates (as in mica) and >429.8 eV for siloxanes (Wagner et al., 1982). In other words, the separation in peaks increases as one goes from silicates to siloxanes. In current studies, the potential for continued contribution from the underlying mica (silicates) to the XPS spectra is significant even after deposition of APTES (siloxanes). In this light, the observed increase in separation of the O 1s and Si 2p peaks after deposition of APTES is in line with a conversion of some Si–O bonds from silanol or silicate forms to siloxane species. This suggests that a covalent siloxane bond forms between the APTES and the mica. Further studies are needed to confirm this result.

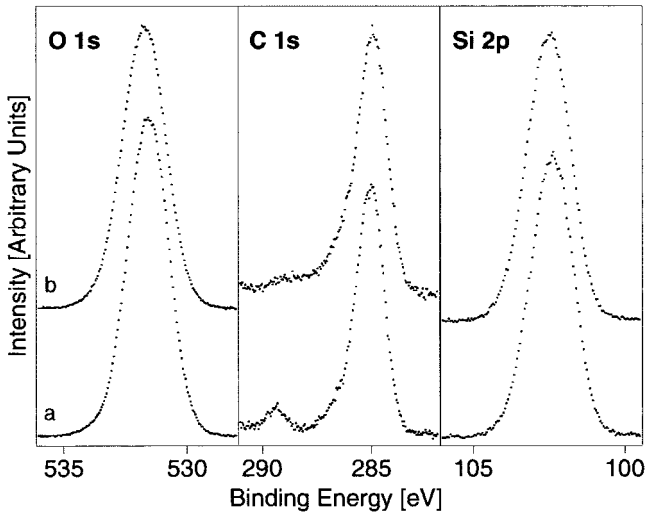

FIGURE 3 High-resolution XPS peaks for three spectral regions on bare mica and AP-mica samples.

The potassium concentration decreases significantly upon any treatment of AP-mica. The deposition of APTES is done via the vapor phase, whereas the depositions of all other compounds (TO and DNA) are performed in solutions. This result suggests, therefore, that potassium may be leached from mica when sample processing is done in solution. One of procedures of DNA immobilization on mica for AFM is based on the use of divalent cations that presumably bridge anionic mica surface and DNA polyanion (Hansma and Laney, 1996). Divalent cations can occupy sites in the mica vacated by potassium ions holding DNA molecules at the surface.

The concentration of nitrogen substantially increases after the treatment of mica with APTES, which is a direct indication of attaching of amino groups to mica surface (the background concentration of nitrogen on bare mica is due to nitrogen absorbed from the atmosphere). Because DNA binds to both types of surfaces (AP-mica and TO-AP-mica), the concentration of nitrogen on the surface increases in all cases (AP-mica vs. DNA/AP-mica and TO-AP-mica vs. DNA/TO-AP-mica). The effect is relatively stronger for AP-mica than for TO-AP-mica, indicating that DNA concentration is potentially higher on the AP-mica than on TO-AP-mica.

One intent of the XPS analysis was to determine whether immobilized amine exists in the active form and to measure the relative amount of immobilized nitrogen (protonated amine) as per Moses et al., 1978, and Nagasaki et al., 1996. The N 1s peaks for all five samples at 90° takeoff angle are shown in Fig. 4. The spectra in Fig. 4 are shown with representative results for a Tougaard baseline (Briggs and Seah, 1990) and peak fitting. Two distinct peaks are seen on all samples. The higher BE component (at ~400 eV) is due to active (protonated) amines and the lower BE component is due to free (unprotonated) amines (Moses et al., 1978; Nagasaki et al., 1996; Briggs and Seah, 1990). The higher BE component can also be due to nitrogen in the amide bond, as supposedly formed after trioxalen binding (step 1 in Fig. 2). Peak fitting was done on N 1s spectra from 90° and 30° takeoff angles for all four modified surfaces. Two peaks, one for active and one for free amine, were used in all cases. Although improvements would be likely in some cases by using three peaks, the nature of the chemistry expected at the sample surfaces does not immediately justify using more than two peaks for the small sample set considered.

The relative amounts of active to free amines was determined from the areas of the two respective N 1s peaks. The results are give in Table 2 as ratios of peak areas for protonated-to-free amine as well as the averages and stan-

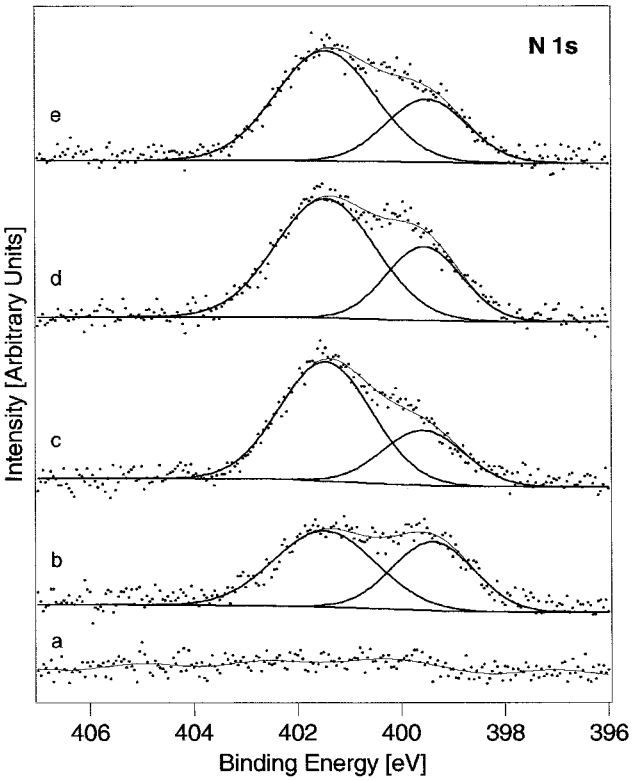

FIGURE 4 High-resolution N 1s spectra for (*a*) bare mica; (*b*)AP-mica; (*c*) TO-mica; (*d*) UV/TO-mica/DNA; and (*e*) AP-mica/DNA taken at 90° takeoff angle. Representative for a Tougaard baseline (Briggs and Seah, 1990) and peak fit results are shown.

dard deviations from the four fitting trials. For the 90° takeoff spectrum of the AP-mica, an additional peak fit was done by reversing the half-widths of the two peaks as starting parameters. This resulted in a significantly different peak area ratio. The results show a trend of increasing protonated-to-free amine going from AP-mica to DNA/AP-mica to TO-AP-mica.

Protonated amines in AP-mica can be in two different configurations, amine-up and amine-down. Due to the nature of the bond formed, the N 1s peak of amine down APTES will overlap with that from protonated amine-up APTES. Assuming all of the APTES molecules are bonded in an amine-up configuration, we would expect the same ratio of protonated-to-free amine peak areas for any takeoff angle because all the amines would be at the outermost interface. Within the limits given by the uncertainty in peak fitting, the results in Table 2 support this model. In other words, amine-up configurations dominate on all three samples represented in Table 2. Some amines may, however, be bonded in an amine-down configuration. Under a conservative assumption that the 30° takeoff angle does not see any of the amine-down bonded APTES, we can calculate an upper limit on the fraction of protonated silane that is potentially bonding in an amine-down configuration based on ratios given in Table 2 at both angles. The maximum amount of APTES in an amine-down bonding configuration is no more than 10% of the total amine density for AP-mica. The actual amount bonded in an amine-down configuration should be (significantly) less than this maximum limit because the K 2p peak from the mica surface is still visible at 30° takeoff angle.

TABLE 2 Ratio of N 1s peak areas for protonated amine relative to free amine

Sample	90°	30°
AP-mica	1.1 ± 0.3	0.9 ± 0.2
AP-mica/DNA	1.9 ± 0.3	1.1 ± 0.3
AP-trioxalen	2.7 ± 0.4	2.8 ± 1.2
UV-DNA	1.8 ± 0.4	1.2 ± 0.1

The conclusions from the ratios in Table 2 are a vast majority, if not all, of the APTES molecules are in an amine-up configuration on all samples, and only ~50% of these amines are active (protonated) on the AP-mica surface. Correspondingly, ~70–75% of the amines in TO-AP-mica are protonated. This effect can be due in part to formation of amide bonds (see Fig. 2) because XPS peaks from amide and alkylamine nitrogens have similar binding energies (Hercules, 1970; Briggs and Seah, 1990). The increase in the relative amount of protonated-to-free amines (from 50% to 70–75%) going from AP-mica to TO-AP-mica suggests a shifting of the equilibrium during the reaction of AP-mica with TFP-trioxalen. This is a direct indication that, once it is immobilized on the mica surface, an amine (free or protonated) is capable of reaction with amine reagents like TFP esters.

AFM imaging of DNA bound to TO-AP-mica

The results from imaging DNA/TO-AP-mica samples are shown in Fig. 5. The DNA concentration in these specific experiments was deliberately high to study the uniformity of the surface modification. The images show a good contrast for DNA molecules, and individual DNA molecules are found even for such high densities of DNA coating. The low magnification image (Fig. 5 *A*) also illustrates that DNA molecules are distributed over the surface quite uniformly, even in the case of such high loadings. The results of control experiments in which the UV irradiation step was omitted are shown in Fig. 6 *A*. There are few if any DNA molecules on the surface. The UV irradiation step was therefore critical for formation of stable UV-induced bonds between TO moieties and DNA. Because SDS treatment removes all weakly adsorbed molecules, these results suggest that photoinduced cross-links are formed between immobilized TO and the DNA bases. A similar effect of SDS was reported in Vandenberg et al. (1991), where immobilization of a number of proteins on aminopropyl surfaces was studied.

The treatment of the specimens of this type with 2 M NaCl solution decreases considerably, but not completely, the number of DNA molecules on the surface. The data in Fig. 6 *B* show that a noticeable amount of DNA molecules

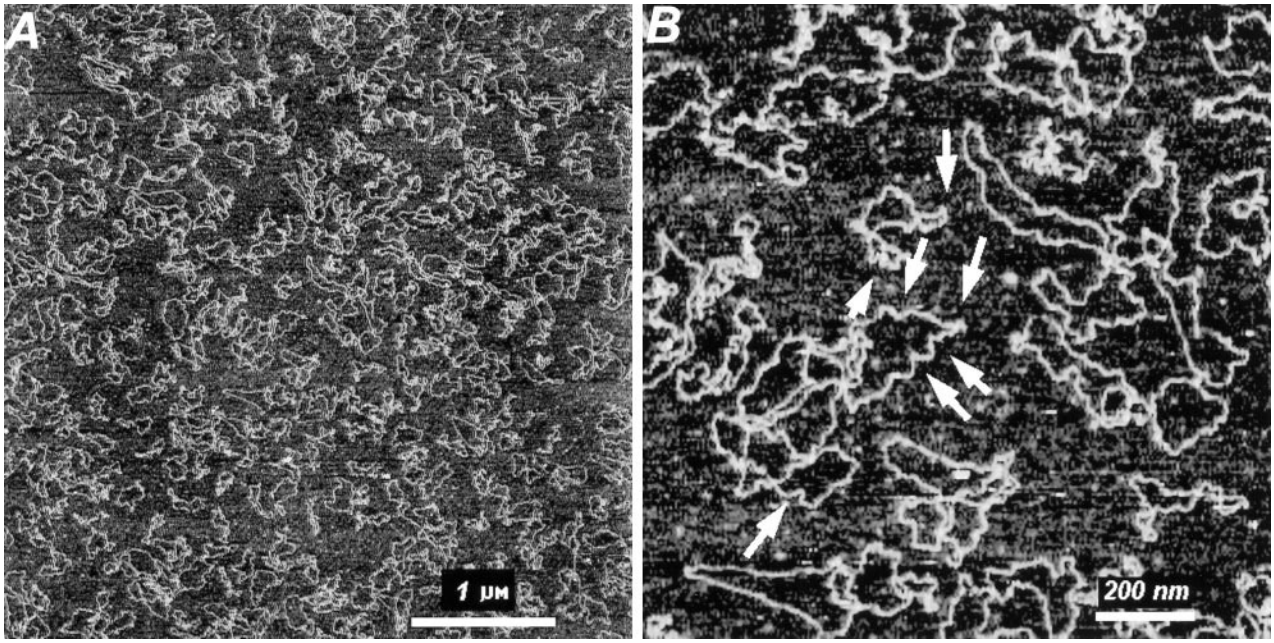

FIGURE 5 AFM images of topologically relaxed plasmid DNA immobilized by photocross-linking to TO-mica. The plate (*B*) is zoomed image of (*A*). Several kinks are indicated with arrows in (*B*). The scan size for the image (*A*) is 4.5 μm.

still remain on the surface. However, the molecules are strongly oriented, suggesting that they interact with the surface rather weakly, so that DNA can be displaced and oriented by the water flow during the rinsing and drying steps. The comparison of effects of SDS and NaCl indicates that both electrostatic and van der Waals forces between DNA and immobilized trioxalen molecules are involved in noncovalent bonding of DNA to TO-mica.

Comparison of images from UV immobilization of DNA/TO-AP-mica with those from direct adsorption of DNA onto AP-mica is instructive. The AFM results for DNA adsorption on AP-mica using the same DNA sample are shown in Fig. 7. The results obtained in parallel experiments for two sample preparation methods (Figs. 5 and 7) reveal two interesting features. They are the coverage of surfaces with DNA molecules and their shape. The coverage of DNA

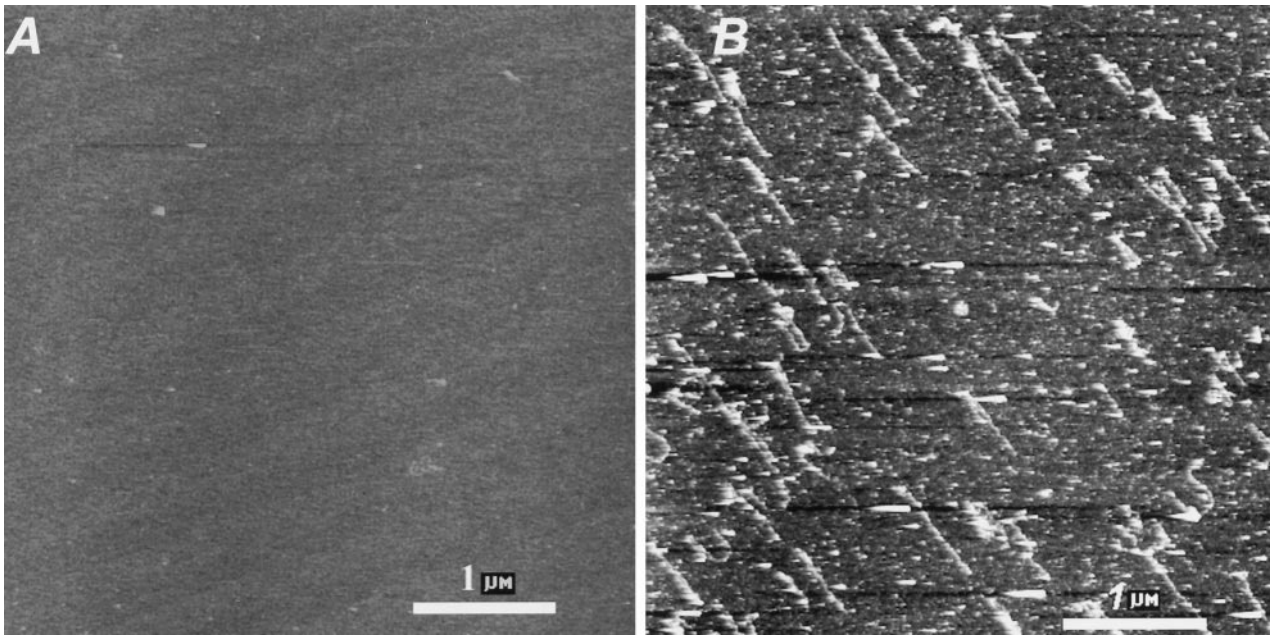

FIGURE 6 AFM images of the samples obtained by deposition of linear plasmid DNA onto TO-mica without UV cross-linking. (*A*) Rinse with 2% SDS and (*B*) rinse with 2 M NaCl. The scan size is 4.5 μm.

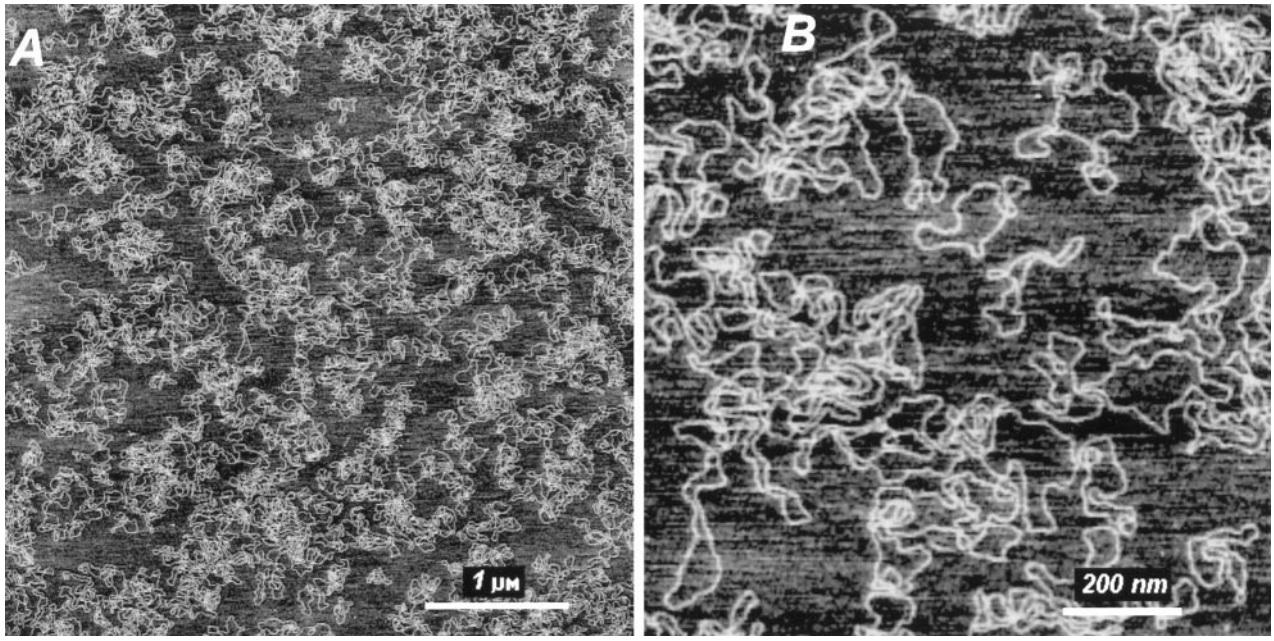

FIGURE 7 AFM images of topologically relaxed plasmid DNA deposited onto AP-mica. Two different scan sizes are shown. The scan size is 4.5 μm.

on AP-mica is considerably higher than that for TO-mica. This suggests that lower numbers of stable contacts are formed between the TO-mica surface and DNA molecules than between AP-mica and DNA molecules. Several factors can explain this difference. First, obtaining 100% reaction of active amino groups with trioxalen esters can be difficult. In addition, immobilization of amino groups should decrease their accessibility for trioxalen moieties. Secondly, stereochemical constraints should be inevitable for interaction of immobilized trioxalen with DNA molecules. Even during reaction of DNA and trioxalen in solution, the number of UV-induced adducts is limited and their stereochemistry controlled by the geometry of the intercalation complex. The length of the spacer between trioxalen molecules and the surface is rather short (a propyl group), so only selected relative orientations of trioxalen and the DNA molecule may lead to the right intercalation of the dye, and thus to formation of stable DNA-trioxalen complexes. Finally, stereochemical constraints may destabilize intercalated complexes, decreasing their concentration. This effect should decrease the number of UV-induced cross-links between trioxalen and DNA.

In addition to circular DNA, linear DNA molecules were deposited onto TO-AP-mica as well. The results are shown in Fig. 8. The image on the top (Fig. 8 *A*) is deposition of linear DNA on AP-mica, and the plate below (Fig. 8 *B*) is the same DNA solution deposited onto TO-AP-mica and UV-cross-linked. The DNA concentration in these experiments was 20 times lower than in the experiments that resulted in supercoiled DNA, and low density of the surface coverage is consistent with this difference.

The DNA molecules on TO-AP-mica surfaces have clear sharp bends or kinks, whereas the geometry of DNA molecules on AP-mica is rather smooth (cf. Figs. 5 *B* and 7 *B* and 8, *A* and *B*, respectively). A few very sharp kinks are indicated in Figs. 5 *B* and 8 *B* with arrows. Intercalated psoralens in addition to monoadducts can form diadducts cross-linking two complementary DNA strands (Cimino et al., 1985). According to crystallographic data (Peckler et al., 1982), psoralen cross-links can bend DNA by as much as

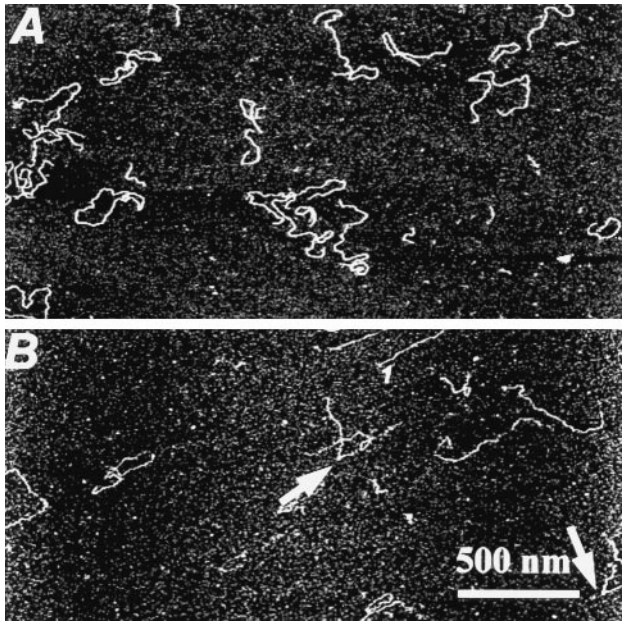

FIGURE 8 AFM images of linearized plasmid DNA deposited on AP-mica (*A*) and immobilized by photocross-linking to TO-mica (*B*). Several kinks in (*B*) are indicated with arrows. One of oriented molecules is marked with Fig. 1. The scan size for both images is 2.6 μm.

70°. Therefore, the kinks on the AFM images are very likely to be the places where interstrand cross-links are formed. In addition, DNA segments between attachment points are moved freely during detergent washing, and this is another factor that can facilitate DNA kinking. Interestingly, oriented DNA molecules can be found in noticeable amounts when linear DNA is immobilized on TO-AP-mica. One such molecule is marked (1) in Fig. 8 *B*. Such molecules were likely attached to the surface at sites close to one end of the DNA. This observation prompts another potential application of TO-AP-mica, namely orienting DNA molecules for various types of physical mapping applications.

The sample in Fig. 5 was supercoiled plasmid DNA with low supercoiling density, and molecules with several intersections are predominately present on the surface. From this point of view, these images are similar to those obtained with AFM for the samples with similar supercoiling density (Shlyakhtenko et al., 1998; cf. Fig. 7). This suggests that no noticeable increase occurs in the number of open circular molecules on the UV-immobilized sample and that this type of sample treatment does not induce formation of single-stranded breaks. Although DNA is transparent in the spectral range used for cross-linking, photoinduced DNA degradation may happen in the psoralen absorption range (Sinden et al., 1980). A rather short irradiation time was chosen in these experiments to avoid undesirable photochemical nicking effects.

CONCLUSIONS

We reported here a procedure for covalent bonding of DNA to a flat mica surface. The DNA molecules are immobilized covalently and thus withstand rinsing with detergents. The functionalized surface remains very smooth during immobilization of the DNA, allowing easy visualization of individual DNA molecules with AFM. The possibility of covalently immobilizing DNA molecules opens realistic prospects for a number of important structural studies.

The covalent immobilization approach promises a number of new avenues for exploration of DNA with AFM. Observations with AFM of the dynamic process of RNA polymerase moving along DNA has recently been demonstrated for weakly bound DNA (Kasas et al., 1997). Covalent attachment of DNA molecules will considerably facilitate such observations on a particular DNA molecule without the fear of the DNA being swept away or moving away during scanning. Having a low number of contacts of the immobilized DNA is beneficial in this case, because more DNA is then accessible for enzymes. Moreover, the immobilization approach presented in the report can be modified in such a way that covalent bonds will be formed only at specific sequences. Psoralen cross-links are introduced preferentially into 5′-TA compared to 5′-AT DNA sequences (Cimino et al., 1985), so this sequence specificity can be used for a corresponding design of the DNA template for a site-specific immobilization. Covalent bonding of DNA also permits performing the experiments with dramatic changes of ionic conditions that may lead to dissociation of one protein and stimulate the binding of another one. Such experiments performed on the same DNA templates may help reveal the role of protein-DNA and protein-protein interactions in specific complex formation. Finally, in addition to topographic studies of DNA, the procedure developed in this report can be applied to study the mechanical properties of immobilized DNA, where attachment of the molecule at one or limited sites is required.

In comparison with double-stranded DNA, the sequence-specific tertiary and secondary structures of RNA are typically single-stranded in nature, are very labile, and depend dramatically on environmental conditions. These factors have considerably limited the application of direct visualization techniques such as AFM to studies of RNA structure. The covalent immobilization of RNA molecules at a limited number of sites should be possible in an analogous manner to that proposed for DNA, and this may help facilitate the imaging of RNA with AFM, in particular in solution conditions.

This report has also shown that AP-mica prepared by modification of mica with APTES at very mild conditions can be used for further surface modification. According to the XPS results, at least 50% of the amines on AP-mica are active (protonated) amines, consistent with the capability of this surface to react with such compounds as tetrafluorphenyl esters. Our preliminary data indicate that AP-mica can be functionalized with succinimide esters as well (Shlyakhtenko, unpublished results), another typical reagent for amines. This suggests that other modifications of AP-mica in addition to the one reported here can be performed.

In summary, AP-mica can be used as a base substrate for modification of surfaces simply by attaching a corresponding active group to the amine after derivatization or by depositing a specific functional silane. Further refinement of the procedures reported here for modification of mica by APTES will lead to the preparation of substrates with a wide range of chemical binding characteristics and almost ideally smooth surface topographies. Such easily tailored substrates will be of great use for future studies of individual biomolecules with AFM.

We are grateful to Drs. E. Henderson and R. Sinden for valuable comments.

This work was supported by National Institutes of Health Grant GM 54991.

REFERENCES

Allen, M. J., X. F. Dong, T. E. O'Neil, P. Yau, S. C. Kowalczykowski, J. Gatewood, R. Balhorn, and E. M. Bradbury. 1993. Atomic force microscope measurements of nucleosome cores assembled along defined DNA sequences. *Biochemistry.* 32:8390–8396.

Bezanilla, M., B. Drake, E. Nudler, M. Kashlev, P. K. Hansma, and H. G. Hansma. 1994. Motion and enzymatic degradation of DNA in the atomic force microscope. *Biophys. J.* 67:2454–2459.

Bezanilla, M., S. Manne, D. E. Laney, Y. L. Lyubchenko, and H. G. Hansma. 1995. Adsorption of DNA to mica, silylated mica, and minerals: characterization by atomic force microscopy. *Langmuir.* 11:655–659.

Brack, C. 1981. DNA electron microscopy. *Crit. Rev. Biochem.* 10: 113–169.

Briggs, D., and M. P. Seah, editors. 1990. Practical Surface Analysis, Vol. 1, 2nd Ed. John Wiley, New York.

Bustamante, C., D. A. Erie, and D. Keller. 1994. Biochemical and structural applications of scanning force microscopy. *Curr. Opin. Struct. Biol.* 4:750–760.

Bustamante, C., and C. Rivetti. 1996. Visualizing protein-nucleic acid interactions on a large scale with scanning force microscope. *Annu. Rev. Biophys. Biomol. Struct.* 25:395–429.

Bustamante, C., J. Vesenka, C. L. Tang, W. Rees, M. Gutfold, and R. Keller. 1992. Circular DNA molecules imaged in air by scanning force microscopy. *Biochemistry.* 31:22–26.

Chrisey, L. A., G. U. Lee, and C. E. O'Ferrall. 1996. Covalent attachment of synthetic DNA to self-assembled films. *Nucleic Acids Res.* 24: 3031–3039.

Cimino, G. D., H. B. Gamper, S. T. Isaacs, and J. E. Hearst. 1985. Psoralens as photoactive probes of nucleic acids structure and functions: organic chemistry, photochemistry, and biochemistry. *Annu. Rev. Biochem.* 54:1151–1193.

Delain, E., and E. Le Cam. 1995. The spreading of nucleic acids. *In* Visualization of Nucleic Acids. G. Morel, editor. CRC Press, Boca Raton. 35–56.

Gamper, H. B., M. W. Reed, T. Cox, J. S. Virosco, A. D. Adams, A. A. Gall, J. K. Scholler, and R. B. Meyer, Jr. 1993. Facile preparation of nuclease resistant 3′ modified oligodeoxynucleotides. *Nucleic Acids Res.* 21:145–150.

Hansma, H. G., and D. E. Laney. 1996. DNA binding to mica correlates with cationic radius: assay by atomic force microscopy. *Biophys J.* 70:1933–1939.

Hansma, H. G., J. Vesenka, C. Siegerist, G. Kelderman, H. Morrett, R. L. Sinsheimer, V. Eilings, C. Bustamante, and P. K. Hansma. 1992. Reproducible imaging and dissection of plasmid DNA under liquid with the atomic force microscopy. *Science.* 256:1180–1184.

Haselgrebler, Th., A. Amerstorfer, H. Schindler, and H. J. Gruber. 1995. Synthesis and applications of a new poly(ethylene glycol) derivative for the crosslinking of amines with thiols. *Bioconjugate Chem.* 6:242–248.

Hegner, M., P. Wagner, and G. Semenza. 1993. Immobilizing DNA on gold via thiol modification for atomic force microscopy imaging in buffer solutions. *FEBS Lett.* 336:452–456.

Herbert, A., M. Schade, K. Lowenkaupt, J. Alfken, T. Schwartz, L. S. Shlyakhtenko, Y. L. Lyubchenko, and A. Rich. 1998. The Zα domain from human ADAR1 binds to the Z-DNA conformer of many different sequences. *Nucleic Acids Res.* 26:3486–3493.

Hercules, D. M. 1970. Electron spectroscopy. *Anal. Chem.* 42:20*a*–40*a*. (Abstr.).

Hinterdorfer, P., W. Baumgartner, H. J. Gruber, K. Schilcher, and H. Schindler. 1996. Detection and localization of individual antibody-antigen recognition events by atomic force microscopy. *Proc. Natl. Acad. Sci. USA*. 93:3477–3481.

Kasas, S., N. H. Thomson, B. L. Smith, H. G. Hansma, X. Zhu, M. Guthold, C. Bustamante, E. T. Kool, M. Kashlev, and P. K. Hansma. 1997. *Escherichia coli* RNA polymerase activity observed using atomic force microscopy. *Biochemistry.* 36:461–468.

Lee, G. U., L. A. Chrisey, C. E. O'Ferrall, D. E. Pilloff, N. H. Turner, and R. J. Colton. 1996. Chemically specific probes for the atomic force microscope. *Israel J. Chem.* 36:81–87.

Lyubchenko, Y. L., R. E. Blankenship, S. M. Lindsay, L. Simpson, and L. S. Shlyakhtenko. 1996. AFM studies of nucleic acids, nucleoproteins and cellular complexes: the use of functionalized substrates. *Scanning Microscopy*. 10(Suppl.):97–109.

Lyubchenko, Y. L., A. A. Gall, L. S. Shlyakhtenko, R. E. Harrington, B. L. Jacobs, P. I. Oden, and S. M. Lindsay. 1992. Atomic force microscopy imaging of dsDNA and RNA. *J. Biomol. Struct. Dyn.* 10:589–606.

Lyubchenko, Y. L., B. L. Jacobs, S. M. Lindsay, and A. Stasiak. 1995. Atomic force microscopy of protein-DNA complexes. Review article. *Scanning Microscopy*. 9:705–727.

Lyubchenko, Y. L., and S. M. Lindsay. 1998. DNA, RNA and nucleoprotein complexes immobilized on AP-mica and imaged with AFM. *In* Procedures in Scanning Probe Microscopy. R. Colton, A. Engel, J. Frommer, H. Gaub, A. Gewirth, R. Guckenberger, J. Rabe, W. Heckl, and B. Parkinson, editors. John Wiley and Sons, Ltd., Chichester, New York, Weinheim, Brisbane, Singapore, Toronto. 493–496.

Lyubchenko, Y. L., S. M. Lindsay, J. A. DeRose, and T. Thundat. 1991. A technique for stable adhesion of DNA to a modified graphite surface for imaging by the STM. *J. Vacuum Sci. Technol.* B9:1288–1290.

Lyubchenko, Y. L., P. I. Oden, D. Lampner, S. M. Lindsay, and K. A. Dunker. 1993. Atomic force microscopy of DNA and bacteriophage in air, water and propanol: the role of adhesion forces. *Nucleic Acids Res.* 21:1117–1123.

Lyubchenko, Y. L., and L. S. Shlyakhtenko. 1997. Visualization of supercoiled DNA with atomic force microscopy in situ. *Proc. Natl. Acad. Sci. USA*. 94:496–501.

Lyubchenko, Y. L., L. S. Shlyakhtenko, T. Aki, and S. Adhya. 1997. AFM visualization of GalR mediated DNA looping. *Nucleic Acids Res*. 25: 873–876.

Lyubchenko, Y. L., L. S. Shlyakhtenko, R. E. Harrington, P. I. Oden, and S. M. Lindsay. 1993. Atomic force microscopy of long DNA: imaging in air and under water. *Proc. Natl. Acad. Sci. USA.* 90:2137–2140.

Mishra, S., and J. J. Weimer. 1995. Comparative analysis of trimethylmethoxysilane and trimethylchlorosilane bonding on polished copper surfaces. *J. Vac. Sci. Technol. A*. 13:1281–1285.

Moses, P. R., L. M. Wier, J. C. Lennox, H. O. Finklea, J. R. Lenhard, and R. W. Murray. 1978. X-ray photoelectron microscopy of alkylaminesilanes bound to metal oxide electrodes. *Anal. Chem*. 50:576–585.

Mou, J., D. M. Czajkowsky, Y. Zhang, and Z. Shao. 1995. High-resolution atomic-force microscopy of DNA: the pitch of the double helix. *FEBS Lett.* 371:279–282.

Nagasaki, Y., J.-Y. Kobayashi, H. Tsujimoto, M. Kato, K. Kataoka, and T. Tsuruta. 1996. The design of a reactive surface with stimuli sensitivity toward temperature and pH. *Nanobiology*. 4:63–70.

Peckler, S., B. Graves, D. Kanne, H. Rapoport, J. E. Hearst, and S. H. Kim. 1982. Structure of a psoralen-thymine monoadduct formed in photoreaction with DNA. *J. Mol. Biol.* 162:157–172.

Pfannschmidt, C., A. Schaper, G. Heim, T. M. Jovin, and J. Langowski. 1996. Sequence-specific labeling of superhelical DNA by triple helix formation and psoralen crosslinking. *Nucleic Acids Res.* 24:1702–1709.

Rabke, C. E., L. A. Wenzler, and T. P. Beebe, Jr. 1994. Electron spectroscopy and atomic force microscopy studies of DNA adsorption on mica. *Scanning Microscopy.* 8:471–480.

Schaper, A., L. I. Pietrasanta, and T. M. Jovin. 1993. Scanning force microscopy of circular and linear plasmid DNA spread on mica with a quaternary ammonium salt. *Nucleic Acids Res*. 21:6004–6009.

Shlyakhtenko, L. S., V. N. Potaman, R. R. Sinden, and Y. L. Lyubchenko. 1998. Structure and dynamics of supercoil-stabilized DNA cruciform. *J. Mol. Biol.* 280:61–72.

Sinden, R. R., J. O. Carlson, and D. E. Pettijohn. 1980. Torsional tension in the DNA double helix measured with trimethylpsoralen in living *E. coli* cells: analogous measurements in insect and human cells. *Cell*. 21:773–783.

Vandenberg, E., H. Elwing, A. Askendal, and I. Lundstrom. 1991. Protein immobilization to 3-aminopropyl triethoxy silane/glutaraldehyde surfaces: characterization by detergent washing. *J. Colloid Interface Sci*. 143:327–335.

Vesenka, J., M. Guthold, C. L. Tang, D. Keller, E. Delaine, and C. Bustamante. 1992. Substrate preparation for reliable imaging of DNA molecules with the scanning force microscopy. *Ultramicroscopy*. 42–44:1243–1249.

Wagner, C. D., D. E. Passoja, H. F. Hillery, T. G. Kinisky, H. A. Six, W. T. Jansen, and J. A. Taylor. 1982. Auger and photoelectron line energy relationship in aluminum oxygen and silicon-oxygen compounds. *J. Vac. Sci. Technol*. 21:933–944.

Yang, J., K. Takeyasu, and Z. Shao. 1992. Atomic force microscopy of DNA molecules. *FEBS Lett.* 301:173–176.